

VIGraph: Self-supervised Learning for Class-Imbalanced Node Classification

Yulan Hu^{1,2}, Sheng Ouyang^{1,2}, Zhirui Yang^{1,2}, and Yong Liu¹

¹ Gaoling School of Artificial Intelligence, Renmin University of China, China

² Kuaishou Technology, China

{huyulan,ouyangsheng,yangzhirui,liuyonggsai}@ruc.edu.cn

Abstract. Class imbalance in graph data poses significant challenges for node classification. Existing methods, represented by SMOTE-based approaches, partially alleviate this issue but still exhibit limitations during imbalanced scenario construction. Self-supervised learning (SSL) offers a promising solution by synthesizing minority nodes from the data itself, yet its potential remains unexplored. In this paper, we analyze the limitations of SMOTE-based approaches and introduce VIgraph, a novel SSL model based on the self-supervised Variational Graph Auto-Encoder (VGAE) that leverages Variational Inference (VI) to generate minority nodes. Specifically, VIgraph strictly adheres to the concept of imbalance when constructing imbalanced graphs and utilizes the generative VGAE to generate minority nodes. Moreover, VIgraph introduces a novel Siamese contrastive strategy at the decoding phase to improve the overall quality of generated nodes. VIgraph can generate high-quality nodes without reintegrating them into the original graph, eliminating the “Generating, Reintegrating, and Retraining” process found in SMOTE-based methods. Experiments on multiple real-world datasets demonstrate that VIgraph achieves promising results for class-imbalanced node classification tasks.

Keywords: graph neural networks, class-imbalanced, auto-encoders

1 Introduction

Node classification is a fundamental task in graph learning across various types of graph data [1,5,20]. Recently, GNNs have demonstrated their ability in dealing with node classification tasks [9,14,25]. However, real-world graph data often exhibits class-imbalance, where the number of nodes in one or more classes is significantly smaller than that in the others, raises the challenge for GNNs. Consequently, there is an urgent need to explore techniques specifically designed for GNNs to address the class-imbalanced scenarios.

The problem of class imbalance has garnered numerous research in traditional machine learning [4,10]. However, due to the non-Euclidean characteristics of graph data, directly applying these methods to graph data is non-trivial.

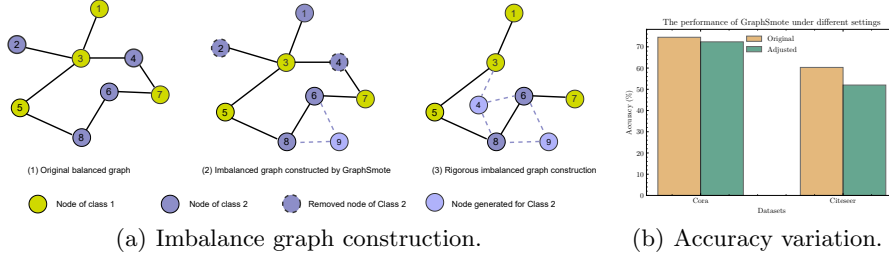


Fig. 1: An explanation of the imbalanced graph construction by GraphSmote and the Accuracy of GraphSmote observed before and after the adjustment of the construction method on Cora and CiteSeer.

The methods tackling the imbalanced problem on graph can be broadly categorized into two categories: re-sampling methods and re-weighting methods. Re-sampling methods address the issue by either increasing the number of samples in minority classes or decreasing the number of samples in majority classes. They synthesize new nodes using SMOTE-based approaches [46]. GraphSmote [47], GraphMixup [42], and GraphENS [34] are representative up-sampling methods. GraphSmote adopts the SMOTE algorithm [6] to perform interpolation between nodes that belong to the minority classes. GraphMixup [42] extends GraphSmote by incorporating self-supervised learning (SSL) to capture structural information and introduces a reinforcement mixup mechanism to determine the upsampling scale, while GraphENS further extends the mixup mechanism to arbitrary nodes via ego graphs. In contrast, ImGCL [45] focuses on down-sampling, gradually reducing the number of majority nodes during the training process. Re-weighting methods address the problem by either altering the loss function to assign more weight to minority classes or adjusting the inference logits for minority classes [26,27,28]. Additionally, ReNode [7] focuses on detecting topological imbalances for individual nodes and adjusts the weights of the identified nodes during the training process.

In this paper, we aim to address the class-imbalanced node classification problem by up-sampling minority nodes. The existing up-sampling methods can be summarized as a three-step process: "Generating, Reintegrating, and Retraining." They utilize up-sampling techniques to generate new nodes, reconnect these nodes to the imbalanced graph, and subsequently retrain the graph using GNNs. However, this paradigm exhibits several limitations.

First, there are critical issues with methods [47,42,34] represented by the SMOTE-based algorithm in constructing imbalanced graphs. Figure 1(a) illustrates the imbalanced graph construction process of these approaches. Due to the lack of imbalanced benchmark graph datasets, the conventional practise involves manually disrupting the node quantity distribution of balanced graphs to obtain imbalanced ones. However, methods [47,42,34] take the original balanced graph as input to obtain node representation. They then remove a proportion

nodes of predefined minority classes to construct the imbalanced scenario. After that, they mixup new nodes based on the node representation learned from the balanced graph. We believe this approach lacks rigorousness, as the node representation trained from a balanced and an imbalanced graph is obviously different due to the distinct message passing within varying graph structures [2]. We propose that the node representation used for up-sampling should be trained on the imbalanced graph to better simulate the realistic scenarios. **Second**, the SMOTE-based methods synthesize minority nodes by performing interpolating between known minority nodes, which can inevitably generate outliers that do not align with the existing minority nodes representation. **Third**, the reintegrating and retraining is time-consuming. The synthesized nodes need to be linked back to the imbalanced graph to obtain balanced graph, which involves measure the distances of each synthesized node from its neighbors. Besides, the balanced graph needs to be retrained for refined embedding.

Based on the above analysis, we pose the following question: **How can we address class-imbalanced node classification on a graph that strictly adheres to the imbalance setting, while generating high-quality minority nodes without necessitating complex designs?** To achieve this, we need to address the following three sub-questions:

How to construct an imbalanced graph that strictly adheres to the imbalance setting? In contrast to SMOTE-based methods, we first disrupt a proportion of nodes to obtain an imbalanced graph. Additionally, we not only remove node features but also remove the edges connected to the discarded nodes, ensuring that these nodes do not participate in message passing. Finally, we encode the imbalanced graph to achieve node representation. In this way, we can maximize the simulation of imbalanced graphs in real-world scenarios and address the shortcomings of SMOTE-based methods. In fact, we conducted comparative experiments based on GraphSmote on Cora and Citeseer. We replaced GraphSmote’s imbalanced graph construction method with the one proposed in this paper, as shown in Figure 1(b), the performance of GraphSmote has declined to varying degrees on both Cora and CiteSeer. *Is there a intuitive method that can serve as the foundation?* The generative SSL models have gain success in the field of Computer Vision (CV) [15,36,37] and Natural Language Processing (NLP) [13,3]. However, its potential for addressing class-imbalanced node classification has not been explored. VGAE [24] represents an early attempt to tackle the link prediction task. In this paper, we employ VGAE as the foundational model to generate minority nodes, ensuring that the generated nodes are learned from the visible nodes. *How to enhance the quality of the generated nodes?* We design comprehensive training strategies to address this concern. We develop a novel Siamese contrastive learning strategy at the decoding phase. This strategy takes effect during decoding, and ultimately forces the encoder to enhance its encoding ability, resulting in higher quality representations. Our contribution can be summarized as: 1) To our best knowledge, this is the first attempt to study generative SSL on class-imbalanced graph node classification. 2) We reexamine the challenge of class-imbalanced node classification, identify-

ing the critical limitations of SMOTE-based methods. 3) We propose VIGraph, a novel SSL model that leverages generative SSL to generate minority nodes and contrastive SSL to enhance the quality of generated nodes. 4) We conduct extensive experiments on multiple real-world datasets, the results validate the effectiveness of VIGraph.

2 Related Work

2.1 Class-Imbalanced Learning on Graphs

The imbalance problem arises from the highly skewed distribution of labels, i.e., the majority class will have a much larger sample size than the minority class, which will lead to sub-optimal performance. The approaches of addressing this problem can be roughly divided into two categories [30]: Re-sampling and Re-weighting.

Re-sampling Approaches The re-sampling approaches aim to balance the distribution of labeled data to tackle the imbalance problem. GraphSMOTE [47] utilizes the SMOTE algorithm to synthesize nodes for the minority classes, and a graph structure reconstruction model is trained to predict the edges of the newly synthesized nodes. However, it is hard to determine the number of nodes to be upsampled for GraphSMOTE. To address this issue, GraphMixup [42] devises a reinforcement mixup mechanism to adaptively determine the number of synthesized minority class nodes. GraphENS [34] synthesizes a new node for the minority classes and its ego graph via the ego graph of a minority class node and an arbitrary node, based on neighbor sampling and saliency-based node mixing. In contrast to the above three methods, which adopt upsampling techniques, ImGCL [45] points out that graph contrastive learning methods are susceptible to imbalanced node classification settings and employs the node centrality based progressively balanced sampling method to balance the distribution of labelled data by decreasing the number of nodes in the majority classes. Generating nodes as well as their topology for the minority classes using the adversarial generation method is a different kind of upsampling method, adopted by ImGAGN [35] and SORAG [12]. In node classification task, where generally only part of the data is labeled, SPARC [48] and SET-GNN [21] expand the set of nodes for the minority classes by assigning pseudo-labels to unlabeled nodes with self-training methods.

Re-weighting Approaches The re-weighting approaches are dedicated to refining algorithms to address the imbalance problem. ACS-GNN [29] modifies the aggregation operation in the standard GNN structure by assigning individual weights to majority class and minority class samples via an attention mechanism, while improving the loss function by utilizing cost-sensitive techniques. ReNode [7] designs a conflict detected-based topology relative location metric (Totoro) to measure the degree of topological imbalance for each node based on which the weight of each node in the loss function is adjusted. TOPAUC [8] is also a reweighting method which utilizes AUC instead of cross entropy as

the loss function since AUC is more suitable for imbalanced data. It devises a topology-aware importance learning (TAIL) mechanism for AUC optimization to adjust the weights of node pairs. TAM [39] designs two components to adjust the logits of the model output, aiming to extend the decision boundary between the minority and majority classes. The first component is the anomalous connectivity-aware margin, which identifies nodes with deviating pattern, based on the local topology of the class pair connectivity. The second component is the anomalous distribution-aware margin, which specifies confusing classes based on neighborhood distribution statistics.

2.2 Generative Self-Supervised Graph Learning

The goal of generative self-supervised learning is to capture the underlying patterns and relationships present in the graph data to facilitate downstream tasks. According to how the reconstruction is performed, generative SSL methods can be grouped into two categories: graph autoencoding methods and graph autoregressive methods [41].

Graph Autoencoding Graph autoencoding performs reconstruction in a one-step manner. GAE and VGAE [24] extends auto-encoder and the variational auto-encoder to graph data incorporating a GCN encoder and a simple inner product decoder. ARGA and ARVGA [32] follow GAE and VGAE adopting graph structure reconstruction, in addition, they force the latent representation to match a prior distribution by an adversarial training scheme. GALA [33] proposes a symmetric graph convolutional autoencoder architecture, which includes a Laplacian smoothing encoder and a Laplacian sharpening decoder as a counterpart of Laplacian smoothing. GMAE [16] focuses on reconstructing node features using masked autoencoder with careful designs, such as masked feature reconstruction, scaled cosine error and Re-mask decoding. HGMAE [40] propose a novel heterogeneous graph masked autoencoder model (HGMAE), which can capture comprehensive structure, attributes and position information from complex heterogeneous graph.

Graph Autoregressive Graph autoregressive methods iteratively execute reconstruction step by step. GraphRNN [44] represents graphs with different node orders as sequences and then builds autoregressive generative models on these sequences. GCPN [43] utilizes reinforcement learning to generate molecular graphs in an autoregressive manner. GPT-GNN [17] introduces an autoregressive framework that iteratively generates node features and edges through two components: attribute generation and edge generation. CCGG [31] is a class-conditional autoregressive graph generation model where class information is incorporated during the generation of the graph structure.

3 Methodology

In this section, we formally present ViGraph. The pre-training phase of our method is depicted in Figure 2, comprising three components: imbalanced graph

construction, pairwise variational encoder, and siamese contrastive decoder. After the pre-training stage, we harness variational inference to generate new nodes that belong to minor classes.

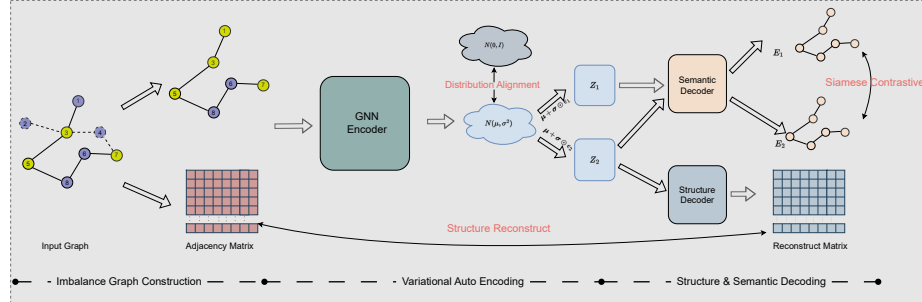


Fig. 2: The Overview of VIGraph. At the outset, the input graph is balanced. To induce an imbalanced graph, specific nodes are selectively discarded, along with their corresponding node features and associated edges. The resultant altered graph is then fed into the encoders to learn the latent variables. To capture distinct aspects of graph information, both a Structure Decoder and a Semantic Decoder are employed.

3.1 Preliminaries

Notations. Given a graph $\mathcal{G} = (\mathcal{V}, \mathcal{E}, \mathcal{X}, \mathcal{Y}, \mathcal{A})$, where \mathcal{V} is the set of N nodes and $\mathcal{E} \subseteq \mathcal{V} \times \mathcal{V}$ is the set of edges. $\mathcal{X} \in \mathbb{R}^{N \times F_s}$, where F_s is the dimension of the input node feature. Each node $v \in \mathcal{V}$ is associated with a feature vector $x_v \in \mathcal{X}$, and each edge $e_{u,v} \in \mathcal{E}$ denotes a connection between node u and node v . $\mathcal{Y} \in \mathbb{R}^n$ represents the class information for the nodes with label information in \mathcal{G} . The graph structure can also be represented by an adjacency matrix $\mathcal{A} \in \{0, 1\}^{N \times N}$ with $A_{u,v} = 1$ if $e_{u,v} \in \mathcal{E}$, and $A_{u,v} = 0$ if $e_{u,v} \notin \mathcal{E}$. For VAE, it usually comprises an encoder f_E , a stochastic latent variable reparameterization module, and a decoder f_D . z_i denotes the stochastic latent variable, summarized as a matrix distribution $\mathbf{Z} \subseteq N \times F'$, where F' is the dimension of the latent variable.

Problem Statement. Suppose there are m node classes $\mathcal{C} = (\mathcal{C}_1, \dots, \mathcal{C}_m)$ in graph \mathcal{G} , where $|\mathcal{C}_i|$ represents the number of nodes in class i . The imbalance ratio, $\frac{\min_i |\mathcal{C}_i|}{\max_i |\mathcal{C}_i|}$, measures class imbalance degree. In the semi-supervised setting, labeled nodes are far fewer than unlabeled ones. We denote labeled set as $\mathcal{D}_L = (\mathcal{V}_L, \mathcal{X}_L, \mathcal{Y}_L)$ and unlabeled set as $\mathcal{D}_U = (\mathcal{V}_U, \mathcal{X}_U, \mathcal{Y}_U)$, with imbalance typically observed in \mathcal{D}_L . Given imbalanced \mathcal{G} and a labeled node subset, VIGraph aims to learn a generator for minority classes. Generated set is denoted as $\mathcal{D}_G = (\mathcal{V}_G, \mathcal{X}_G, \mathcal{Y}_G)$. Augmenting \mathcal{D}_L with \mathcal{D}_G forms $\mathcal{D}_S = \mathcal{D}_L \cup \mathcal{D}_G$, achieving

a balanced distribution in the updated set \mathcal{D}_S . Network $\Psi : \mathcal{V} \rightarrow \mathcal{Y}$ is trained on \mathcal{D}_S and can further predict labels on the unlabeled set \mathcal{D}_U .

3.2 Imbalanced Graph Construction

As discussed in Section 1, previous SMOTE-based up-sampling approaches for imbalanced node classification can be summarized into three steps. **Generating:** First, the original balanced graph \mathcal{G} is encoded into representation \mathcal{H} . Subsequently, a subset of classes is selected as minority classes (denoted as C_m), with a portion of nodes in C_m designated as minority nodes, resulting in an imbalanced graph $\bar{\mathcal{G}}$. The mixup interpolation is then performed between minority nodes based on \mathcal{H} , generating minority nodes \mathcal{V}_N . **Reintegrating:** Distances between the generated nodes \mathcal{V}_N and the nodes in $\bar{\mathcal{G}}$ are calculated. If the distance is smaller than a predefined threshold, an edge is created, yielding a balanced graph denoted as $\tilde{\mathcal{G}}$. **Retraining:** $\tilde{\mathcal{G}}$ is further encoded into representation $\tilde{\mathcal{H}}$, which will be used for downstream node classification.

We assert the construction process, especially the minor node generation, is problematic. On one hand, the embedding for generating minority class nodes should be based on the constructed imbalanced graph $\tilde{\mathcal{G}}$ rather than the original balanced graph \mathcal{G} . However, previous SMOTE-based methods utilize \mathcal{H} for feature interpolation. On the other hand, due to the impact of message passing during graph encoding, when encoding the imbalanced graph, the characteristics of the discarded nodes (node features and the edges connected to it) should be completely removed, however, the previous SMOTE-based methods did not eliminate this impact, which resulted in biased node representations used for generating new nodes.

In contrast to previous methods, we introduce a more rigorous approach to construct the imbalanced graph. We begin by constructing the imbalanced graph first and then proceed to encode it for graph embedding. Moreover, we not only remove the nodes but also eliminate their associated features and connecting edges. As a result, the constructed imbalanced graph represents a subgraph of the original graph. This process guarantees the complete absence of discarded nodes and their features at all stages, thereby adheres strictly to the actual imbalanced scenario. For simplicity, we will not explicitly delve into the distinction between the original graph and the constructed subgraph in the subsequent sections. By default, we will refer to the subgraph as the graph.

3.3 Variational Graph Autoencoder

Stochastic Properties Encoding. VIGraph employs a single-layer GNN to encode the imbalanced graph:

$$\mathcal{H} = \text{ReLU}(\text{GNN}(\mathcal{A}\mathcal{X}\mathcal{W})), \quad (1)$$

where $\text{ReLU}(\cdot) = \max(0, \cdot)$, $\mathcal{H} \in \mathbb{R}^{\mathcal{N} \times F_d}$, F_d is the hidden feature dimension of \mathcal{H} , \mathcal{W} is the weight matrix. Then we focus on learning the posterior distribution $p_\theta(\mathbf{Z}|\mathcal{H}, \mathcal{A})$ for latent variable \mathbf{Z} generation. Here, z_i represents the latent variable of node i . To achieve this, we introduce two auxiliary GNN layers, GNN_μ and GNN_σ , to independently learn the mean and variance representation of \mathcal{H} , denoted as μ and σ . Due to the intractability of computing the true posterior, we introduce a new approximation function q_ϕ , parameterized by ϕ , to output an approximation given input \mathcal{H} and \mathcal{A} [23]. Following VGAE [23], we use a variational distribution in the form of:

$$q(\mathbf{Z} | \mathcal{H}, \mathbf{A}) = \prod_{i=1}^N q(\mathbf{z}_i | \mathcal{H}, \mathbf{A}) = \prod_{i=1}^N \mathcal{N}(\mathbf{z}_i | \boldsymbol{\mu}_i, \boldsymbol{\sigma}_i). \quad (2)$$

Pairwise Reparameterization. After obtaining the mean and variance of the latent variables, we employ the reparameterization technique [23] to sample from the latent variables. Specifically, sampling from the variational posterior $z_i \sim p(z_i | \mathcal{H}, \mathcal{A})$, is equivalent to sampling from a standard normal distribution:

$$\mathbf{z}_i = \boldsymbol{\mu}_i + \boldsymbol{\sigma}_i \odot \epsilon; \epsilon \sim \mathcal{N}(0, 1), \quad (3)$$

where \odot denotes element-wise multiplication and ϵ is a sample from the standard normal distribution.

Unlike the common practice, we adopt a novel and straightforward strategy to perform pairwise reparameterization, obtaining two latent variables for cross-view contrastive learning at decoding phase, which we will elaborate in Section 3.4. Specifically, this strategy involves randomly sampling two variables from a standard normal distribution, then generate new representations following Equation 3, resulting in the latent representation Z_1 and Z_2 . In fact, given the stochastic variable of the target nodes, VIGraph can generate an arbitrary number of new latent representation. This idea serves as the foundation for our approach to generating samples for minority classes.

To ensure the closeness between the real posterior $p_\theta(\mathbf{Z}|\mathcal{H}, \mathcal{A})$ and approximation posterior $q_\phi(\mathbf{Z}|\mathcal{H}, \mathcal{A})$, we use Kullback-Leibler (KL) divergence to quantify the distance between the two distributions. The Evidence Lower Bound (ELBO) is defined as follows:

$$\mathcal{L}_{elbo} = \mathbb{E}_{z \sim q_\phi(\mathbf{Z}|\mathcal{H}, \mathcal{A})} \log p(\mathcal{H} | \mathbf{Z}) - D_{KL}(q_\phi(\mathbf{Z} | \mathcal{H}, \mathcal{A}) \| p_\theta(\mathbf{Z})). \quad (4)$$

3.4 Structure and Semantic Decoders

The GAEs commonly employ a reconstruction criterion to capture the inherent characteristics of the input graph. The configuration of the decoder varies based on downstream tasks [23,16,40]. The Mean Squared Error (MSE) is often adopted as the loss criterion. However, due to the sparsity of the input features, the MSE value can result in extremely low magnitudes of loss values, making it impractical for effective training. As a result, directly adopting the MSE as

the loss criterion for feature reconstruction is not suitable. To fully exploit the underlying semantic information while preserving the structural details, we introduce a structure decoder and a feature decoder to address the structural and semantic information, respectively.

Structure Reconstruction To preserve the structural information, we aim to recover the adjacency matrix from the decoded output and compare it with \mathcal{A} . To achieve this, we employ a simple inner dot product as the structure decoder. Denoting the decoded outcome as \hat{X} , the reconstruction procedure is formulated as follows:

$$\hat{A}_{v,u} = \rho(\hat{x}_v \cdot \hat{x}_u^T), \quad (5)$$

where \hat{A} signifies the reconstructed adjacency matrix and $\hat{A}_{v,u}$ indicates the connectivity between nodes u and v . The function ρ corresponds to the sigmoid activation function. By translating the reconstruction task into a binary classification problem, we employ the cross-entropy (CE) loss to quantify the difference between \mathcal{A} and \hat{A} . The inter-node connectivity effectively serves as an indicator of the class, with the two classes denoted by 0 and 1. Due to the sparsity, the number of positive samples (class 1) in the graph significantly outweighs the number of negative samples. To address this imbalance, we adopt a weighted version of the CE loss. For each row r in the adjacency matrix \mathcal{A} , the weight assigned to the positive sample i is computed as $\mathbf{W}_i = (N - P_{ri})/P_{ri}$, where P_{ri} represents the number of positive samples in row r . The final reconstruction loss is computed as follows:

$$\mathcal{L}_{\text{rec}} = -\frac{1}{N^2} \sum_{i=1}^{N^2} \left[\mathbf{W}_i \mathcal{A}_i \ln \hat{A}_i + (1 - \mathcal{A}_i) \ln(1 - \hat{A}_i) \right], \quad (6)$$

Siamese Contrastive Decoding As a self-supervised method, the improvement of semantic decoding quality can in turn force the encoder to generate better representation. The context-based contrastive learning strives to enhance the congruence at the node level between the decoded embeddings. Here, we employ a single-layer MLP as the feature decoder. Once the reparameterized latent embeddings Z_1 and Z_2 are generated, they are subsequently decoded into $\tilde{\mathbf{X}}_1$ and $\tilde{\mathbf{X}}_2$, respectively:

$$\tilde{X}_1 = \text{ReLU}(\text{MLP}(Z_1)), \tilde{X}_2 = \text{ReLU}(\text{MLP}(Z_2)). \quad (7)$$

In essence, the two decoded embeddings can be regarded as Siamese views [49]. In particular, we need to consider both inter-view and intra-view contrastiveness. For a single node x_i , its embedding generated in the first view, denoted as \tilde{x}_1 , serves as the anchor. The embedding of the same node generated in the second view, denoted as \tilde{x}_2 , represents the positive sample. The embeddings of other nodes in both views are considered as negative samples. In this way, the positive pair can be denoted as $(\tilde{x}_1, \tilde{x}_2)^+$, the negative pairs can be denoted as $(\tilde{x}_1, \tilde{v}_1)^- \cup (\tilde{x}_1, \tilde{v}_2)^-$, where \tilde{v} indicates the embedding of node in the Siamese views.

To quantify the relationship between these embeddings, we introduce a cosine similarity function $\eta(\tilde{x}_1, \tilde{x}_2)$ to calculate the similarity score between nodes in separate views. Formally, we define the pairwise objective for each positive pair $(\tilde{x}_1, \tilde{x}_2)$ as follows:

$$\begin{aligned} \mathcal{L}_{gcl}(\tilde{x}_1, \tilde{x}_2) &= \log \frac{e^{\theta(\tilde{x}_1, \tilde{x}_2)/\tau}}{\underbrace{e^{\theta(\tilde{x}_1, \tilde{x}_2)/\tau}}_{\text{the positive pair}} + \underbrace{\sum_{k=1}^N \mathbb{1}_{[k \neq i]} e^{\theta(\tilde{x}_1, \tilde{x}_2)/\tau}}_{\text{inter-view negative pairs}} + \underbrace{\sum_{k=1}^N \mathbb{1}_{[k \neq i]} e^{\theta(\tilde{x}_1, \tilde{x}_2)/\tau}}_{\text{intra-view negative pairs}}}, \end{aligned} \quad (8)$$

where τ indicates the temperature value.

3.5 Minority Node Generation

Upon concluding the pre-training phase, our approach initiates an iterative reparameterization process based on the learned stochastic latent variables μ and σ according to Equation 3, continuing until the number of samples in each class reaches equilibrium.

The quality of the generated samples is ensured through two main considerations. Firstly, the newly generated samples are created based on the stochastic characteristics of the existing minority samples. This ensures that the distribution of the newly generated samples aligns with that of the existing minority samples, preventing potential outliers that could arise from convex combinations of node features. Secondly, the well-designed training strategy guarantees a comprehensive exploration of the graph's features, allowing the newly generated samples to closely resemble the original graph. In contrast to prior methods [47, 42, 34] that link the nodes in \mathcal{D}_G back to the graph for further training, we directly integrate the generated nodes into the original labeled set \mathcal{D}_L , resulting in a unified set denoted as \mathcal{D}_S . For performance assessment, we employ a simple logistic regression classifier on \mathcal{D}_S to make predictions on the test set.

3.6 Training and Optimization

Altogether, we jointly optimize both the ELBO and structure reconstruction losses in addition to the Siamese contrastive loss. We define the final optimization function as follows:

$$\mathcal{L} = \alpha \mathcal{L}_{elbo} + \beta \mathcal{L}_{rec} + \gamma \mathcal{L}_{gcl}, \quad (9)$$

where α , β and γ are hyper-parameters which mediate the strengths of each loss term.

4 EXPERIMENTS

In this section, we conduct extensive experiments with the aim of answering the following three research questions (RQ): **RQ1**: How does the VIGraph perform

compare against other SOTA methods? **RQ2**: Does VIGraph exhibit robustness across varying class-imbalance ratios? **RQ3**: How do distinct components and parameters influence the overall performance of the model?

4.1 Experimental Setups

To comprehensively illustrate the efficacy of VIGraph, we conduct experiments on five real-world datasets. Cora, CiteSeer, and PubMed [25] are three citation network datasets. Following the method elucidated in [47,7], for each dataset, we designate half of the available classes as minority classes. We then reduce the number of nodes within the minority classes in accordance with the prescribed imbalance ratio, denoted as λ . Assuming the dataset encompasses $|\mathcal{C}|$ labeled classes, each containing N_c nodes, we select $\frac{|\mathcal{C}|}{2}$ classes as minority classes, with $\lambda \times N_c$ nodes assigned to each respective minority class. In addition, we adopt the co-purchase graph AmazonPhoto [38] and the Wikipedia-based graph Wiki-CS [19] to further evaluate VIGraph. AmazonPhoto contains eight classes with varying numbers. We choose four of the eight classes that contain relatively fewer samples and manually set the number of these four classes to 10% of the number of classes with the most samples. For Wiki-CS, following the approach detailed in GraphMixup [42], we identify classes with fewer samples than the average as minority classes.

Baselines To evaluate the universality and stability of VIGraph, we choose GCN [25] and GraphSage [14] as the backbone model for VIGraph. The following seven SOTA methods of four groups are chosen for comparison:

- **CE**(Cross Entropy loss). Use CE as a loss function on the backbone model.
- **RW**(Re-Weight loss) [18], **FC**(Focal loss) [28] and **CB**(Class Balanced loss) [11] are three re-weighting methods based on losses.
- **ReNode** [7] is a re-weighting method according to the degree of nodes’ topological.
- **GraphSMOTE** [47] and **GraphMixup** [42] are two upsampling methods.

For VIGraph, we present two variants denoted as $\text{VIGraph}^{\spadesuit}$ and $\text{VIGraph}^{\clubsuit}$. $\text{VIGraph}^{\spadesuit}$ construct the imbalance graph align with previous works like GraphSmote [47] and GraphMixup [42], which we believe not rigorous. Conversely, $\text{VIGraph}^{\clubsuit}$ rigorously adheres to the definition of imbalance.

Setting Aligned with existing work, we selected three widely used evaluation metrics: accuracy (**Acc**), balanced accuracy (**bAcc**), and macro F-score (**F1**). The hidden dimension is set to 128, while the output dimension is configured as 64. For optimization, we employ the Adam optimizer [22] with the learning rate search between 0.0005 and 0.01. The maximum number of training epochs is set at 1000. All experiments are conducted on a single NVIDIA V100 32GB GPU. The presented results are performed ten times to compute the average and standard deviation.

Table 1: Experimental results on Cora, CiteSeer, PubMed, AmazonPhoto and Wiki-CS datasets. The best results are marked bold and the second best result is underlined.

Dataset	Backbone	Metric	CE	RW	FC	CB	GS	RN	GM	V^\spadesuit	V^\clubsuit
Cora	GCN	Acc	63.42 \pm 1.14	<u>75.00</u> \pm 1.19	65.52 \pm 1.92	71.88 \pm 3.48	74.54 \pm 1.43	72.20 \pm 1.92	74.54 \pm 0.45	77.60 \pm 0.77	78.47 \pm 1.05
		bAcc	60.18 \pm 1.02	<u>75.76</u> \pm 1.01	61.65 \pm 1.71	73.10 \pm 3.12	75.11 \pm 1.52	73.74 \pm 2.32	74.61 \pm 0.40	78.70 \pm 0.94	79.13 \pm 0.96
		F1	51.29 \pm 3.58	73.81 \pm 0.76	55.27 \pm 4.52	71.76 \pm 2.44	73.10 \pm 1.16	71.36 \pm 2.36	<u>74.55</u> \pm 0.21	76.67 \pm 0.93	77.66 \pm 1.08
	SAGE	Acc	72.94 \pm 3.25	74.42 \pm 0.56	74.26 \pm 1.53	73.66 \pm 2.04	72.46 \pm 0.21	73.04 \pm 1.23	<u>76.10</u> \pm 0.10	78.70 \pm 0.92	79.22 \pm 1.02
		bAcc	73.79 \pm 2.12	<u>74.90</u> \pm 0.48	74.22 \pm 1.80	73.65 \pm 2.77	72.38 \pm 1.97	73.29 \pm 1.35	-	78.92 \pm 0.49	79.76 \pm 1.03
		F1	72.06 \pm 2.92	72.48 \pm 0.48	72.74 \pm 1.81	71.59 \pm 2.04	70.52 \pm 0.16	72.13 \pm 1.03	75.8 \pm 0.20	77.64 \pm 1.12	78.64 \pm 0.80
	CiteSeer	Acc	53.74 \pm 1.44	61.40 \pm 1.85	53.02 \pm 5.45	61.76 \pm 3.92	60.30 \pm 2.37	57.58 \pm 2.49	62.40 \pm 0.53	65.60 \pm 0.38	66.26 \pm 0.52
		bAcc	52.77 \pm 0.77	<u>58.55</u> \pm 1.34	51.91 \pm 4.94	58.26 \pm 3.64	55.57 \pm 2.09	53.05 \pm 2.36	57.18 \pm 0.47	61.29 \pm 0.63	61.49 \pm 0.47
		F1	51.02 \pm 1.82	57.33 \pm 1.81	48.70 \pm 7.82	56.54 \pm 5.57	53.04 \pm 2.55	53.05 \pm 2.36	58.39 \pm 0.46	60.55 \pm 0.77	60.86 \pm 0.59
PubMed	GCN	Acc	37.08 \pm 16.95	43.88 \pm 22.16	49.90 \pm 17.22	59.44 \pm 1.44	59.42 \pm 1.31	60.28 \pm 0.49	64.70 \pm 0.35	66.02 \pm 0.80	66.46 \pm 1.01
		SAGE	33.98 \pm 17.82	54.34 \pm 2.91	47.78 \pm 15.73	55.33 \pm 1.30	54.95 \pm 1.14	55.58 \pm 1.08	59.76 \pm 0.23	62.72 \pm 0.70	63.46 \pm 1.41
		F1	26.98 \pm 22.60	52.84 \pm 2.99	43.98 \pm 19.88	53.76 \pm 2.06	51.91 \pm 1.68	52.98 \pm 1.67	61.88 \pm 0.72	62.06 \pm 0.82	62.58 \pm 1.58
	SAGE	Acc	75.30 \pm 0.36	74.60 \pm 0.97	74.90 \pm 1.32	74.58 \pm 0.32	73.90 \pm 1.07	73.58 \pm 0.20	76.25 \pm 0.50	77.48 \pm 0.55	77.86 \pm 0.75
		bAcc	72.99 \pm 0.79	74.11 \pm 0.77	74.61 \pm 1.33	74.55 \pm 0.61	71.84 \pm 0.82	70.22 \pm 0.65	74.16 \pm 0.35	77.09 \pm 0.38	78.2 \pm 0.85
		F1	74.38 \pm 0.45	74.29 \pm 0.92	<u>74.66</u> \pm 1.17	74.34 \pm 0.39	72.99 \pm 0.78	72.17 \pm 0.52	73.10 \pm 0.66	76.70 \pm 0.55	77.13 \pm 0.75
	Photo	Acc	73.66 \pm 1.15	73.86 \pm 0.50	73.48 \pm 0.37	73.82 \pm 0.53	72.72 \pm 0.61	72.52 \pm 0.69	76.50 \pm 0.22	79.77 \pm 0.62	79.28 \pm 0.65
		bAcc	73.66 \pm 2.66	73.61 \pm 0.33	73.40 \pm 0.41	74.28 \pm 0.70	69.95 \pm 1.70	68.80 \pm 0.87	<u>75.57</u> \pm 0.49	79.61 \pm 0.39	78.90 \pm 0.76
		F1	72.83 \pm 1.43	73.59 \pm 0.51	73.41 \pm 0.35	73.54 \pm 0.42	71.51 \pm 0.81	70.97 \pm 0.85	76.10 \pm 0.10	78.83 \pm 0.57	78.41 \pm 0.69
Wiki-CS	GCN	Acc	87.55 \pm 1.61	88.29 \pm 5.12	85.53 \pm 0.3	90.43 \pm 0.41	91.8 \pm 0.78	88.58 \pm 2.4	89.19 \pm 1.12	91.96 \pm 1.12	92.34 \pm 0.83
		bAcc	81.27 \pm 3.67	88.67 \pm 2.22	80.94 \pm 0.48	87.95 \pm 0.46	90.23 \pm 1.24	84.82 \pm 3.23	88.75 \pm 1.76	89.58 \pm 2.05	89.74 \pm 1.61
		F1	82.85 \pm 3.47	87.25 \pm 4.01	81.31 \pm 0.42	88.09 \pm 0.45	89.21 \pm 1.35	85.38 \pm 3.34	86.25 \pm 2.01	90.22 \pm 1.90	90.57 \pm 1.40
	SAGE	Acc	91.45 \pm 0.81	86.35 \pm 1.29	38.47 \pm 26.61	66.45 \pm 28.33	88.57 \pm 1.32	-	90.54 \pm 0.94	92.20 \pm 0.94	92.40 \pm 1.19
		bAcc	87.16 \pm 1.27	79.26 \pm 2.5	27.73 \pm 30.46	57.06 \pm 33.18	84.77 \pm 1.57	-	90.12 \pm 1.22	90.16 \pm 1.19	90.65 \pm 1.80
		F1	89.04 \pm 1.25	82.66 \pm 2.12	21.86 \pm 33.68	55.64 \pm 37.83	86.26 \pm 1.6	-	89.66 \pm 0.86	90.88 \pm 0.83	91.38 \pm 1.27
	GCN	Acc	70.87 \pm 0.17	66.47 \pm 0.51	70.66 \pm 0.1	71.36 \pm 0.36	67.23 \pm 0.43	70.57 \pm 0.22	<u>77.96</u> \pm 0.41	79.44 \pm 0.42	-
		bAcc	63.08 \pm 0.18	65.34 \pm 0.52	63.74 \pm 0.31	63.97 \pm 0.53	65.42 \pm 0.27	62.74 \pm 0.32	<u>74.65</u> \pm 0.23	76.20 \pm 0.70	-
		F1	67.88 \pm 0.06	65.66 \pm 0.48	68.35 \pm 0.26	68.36 \pm 0.70	66.87 \pm 0.57	67.25 \pm 0.27	<u>73.63</u> \pm 0.48	77.03 \pm 0.42	-
	SAGE	Acc	82.03 \pm 0.1	80.77 \pm 0.17	<u>81.22</u> \pm 0.07	81.05 \pm 0.14	80.36 \pm 0.36	80.13 \pm 0.16	79.20 \pm 0.02	79.48 \pm 0.39	-
		bAcc	79.17 \pm 0.08	80.25 \pm 0.51	78.51 \pm 0.21	79.36 \pm 0.15	78.37 \pm 0.30	76.78 \pm 0.44	-	76.09 \pm 0.64	-
		F1	79.41 \pm 0.08	78.77 \pm 0.24	78.84 \pm 0.22	<u>78.99</u> \pm 0.26	78.28 \pm 0.35	77.15 \pm 0.33	76.40 \pm 0.02	77.00 \pm 0.55	-

4.2 Class-Imbalanced Classification (RQ1)

To answer **RQ1**, we evaluate the VIGraph on four datasets, and compare the results with seven SOTA methods. Table 1 presents the evaluation results, with the best-performing models marked in bold and the second-best results marked with underline. To fit the page size, we employ aliases for the methods under consideration: GS represents GraphSmote, RN corresponds to ReNode, GM signifies GraphMixup, V^\spadesuit is an abbreviation for VIGraph $^\spadesuit$, and V^\clubsuit denotes VIGraph $^\clubsuit$. The performance of all compared baselines are listed if they are reported in the original paper, otherwise we reproduce the results by following the code provided in the paper. When reproducing ReNode with Graphsage as the backbone model, we encountered the gradient vanishing problem, we leave the corresponding space as “-”. Besides, Please note that GraphMixup use GraphSage as the backbone model and did not report the result of balanced accuracy, so we leave the corresponding space as “-”.

We can draw three observations from Table 1. Firstly, VIGraph $^\spadesuit$ outperforms all other baselines by a significant margin except on the Wiki-CS dataset, where GraphSage serves as the backbone model. VIGraph $^\spadesuit$ achieved an average improvement of 1.97% to the second-best results across the five datasets in terms of Accuracy. Moreover, since the Wiki-CS dataset is originally imbalanced, there is no need to manually create the imbalanced setting. As a result, the performance

Table 2: Ablation Studies of three training losses on Cora, CiteSeer and PubMed.

Dataset	Cora			CiteSeer			PubMed			
	Metric	Acc	bACC	F1	Acc	bACC	F1	Acc	bACC	F1
V^{\spadesuit}		77.60	78.70	76.67	65.60	61.29	60.55	77.48	77.09	76.70
w.o. \mathcal{L}_{rec}		76.30	77.42	75.44	63.78	63.11	61.26	75.02	75.21	74.35
w.o. \mathcal{L}_{elbo}		77.00	78.48	76.77	65.08	60.92	60.54	76.64	76.79	76.08
w.o. \mathcal{L}_{gcl}		75.48	76.77	75.01	63.02	59.79	59.2	75.34	75.62	74.73

of VIGraph on Wiki-CS does not exhibit a distinction between V^{\spadesuit} and V^{\clubsuit} . Secondly, VIGraph demonstrates effectiveness across different backbone models, showcasing its universality and stability. Thirdly, VIGraph $^{\clubsuit}$ achieved even higher performance than VIGraph $^{\spadesuit}$, surpassing the second-best result by 2.47% across the five datasets in terms of Accuracy. This observation not only proves that preserving graph characteristics significantly contributes to enhancing the model’s learning capacity, but also suggests that the existing SOTA methods might have limitations in terms of graph construction.

4.3 Classification Under different Imbalance Ratio (RQ2)

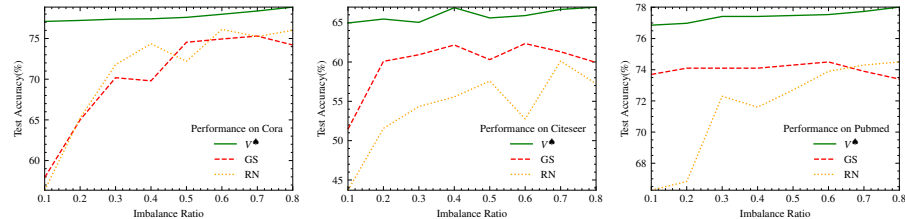


Fig. 3: The performance across various imbalance rates.

We conducted experiments on Cora, CiteSeer, and PubMed under different imbalance ratios to address **RQ2**. We selected GraphSmote and ReNode for comparison. GraphSmote is a representative upsampling method, while ReNode focuses on re-weighting the loss for different nodes.

To investigate the impact of different imbalance ratios (λ), we varied λ from 0.1 to 0.8 with a step size of 0.1. A λ value of 0.1 indicates an extremely imbalanced graph, while a value of 0.8 indicates a graph close to a balanced setting.

From Figure 3, we can observe two key findings. First, VIGraph consistently outperformed GraphSmote and ReNode across various imbalance ratios, demonstrating the universal superiority of VIGraph. Second, all models were affected by the imbalance setting, but VIGraph maintained relatively stable performance

even when the graph exhibit extremely imbalance. This highlights the robustness of VIGraph and showcases its ability to generate high-quality samples that compensate for the lack of minority nodes. Overall, the experimental results demonstrate the superior performance, robustness, and stability of VIGraph under different imbalance ratios.

4.4 Ablation Studies (RQ3)

We explore the influence of training losses to answer **RQ3**. Table 2 presents the results of the ablation studies performed on the Cora, Citeseer, and Pubmed. GCN is used as the backbone model. The results validate the positive contribution of all three training strategies to the model’s performance. However, it is important to note that the impact of each strategy varies across the different datasets. This observation suggests that each strategy plays a distinct role in the context of different datasets, highlighting the importance of considering dataset-specific characteristics when designing training strategies.

5 CONCLUSION AND DISCUSSION

In this paper, we focus on addressing the class-imbalanced problem in node classification. We analyze the limitations of existing representative methods, particularly their improper construction of imbalanced graph. We propose VIGraph, an generative self-supervised approach that integrates generative learning with contrastive learning to effectively generate nodes for the minority class. We introduce several key training strategies to enhance the overall performance of VIGraph. These strategies are designed to comprehensively capture both semantic and structural information on the graph, facilitating the generation of high quality minority nodes. We conduct extensive experiments on four real-world datasets, the superior performance demonstrate the effectiveness and robustness of VIGraph. Furthermore, we conduct thorough ablation studies to provide additional insights into the individual efficacy of each training strategy employed in VIGraph. We will continue to explore more applications of the generative model to graph tasks.

References

1. Arora, S.: A survey on graph neural networks for knowledge graph completion. arXiv preprint arXiv:2007.12374 (2020)
2. Balcilar, M., Héroux, P., Gauzere, B., Vasseur, P., Adam, S., Honeine, P.: Breaking the limits of message passing graph neural networks. In: International Conference on Machine Learning. pp. 599–608. PMLR (2021)
3. Brown, T., Mann, B., Ryder, N., Subbiah, M., Kaplan, J.D., Dhariwal, P., Neelakantan, A., Shyam, P., Sastry, G., Askell, A., et al.: Language models are few-shot learners. Advances in neural information processing systems **33**, 1877–1901 (2020)
4. Buda, M., Maki, A., Mazurowski, M.A.: A systematic study of the class imbalance problem in convolutional neural networks. Neural networks **106**, 249–259 (2018)

5. Cai, D., Shao, Z., He, X., Yan, X., Han, J.: Mining hidden community in heterogeneous social networks. In: Proceedings of the 3rd international workshop on Link discovery. pp. 58–65 (2005)
6. Chawla, N.V., Bowyer, K.W., Hall, L.O., Kegelmeyer, W.P.: Smote: synthetic minority over-sampling technique. *Journal of artificial intelligence research* **16**, 321–357 (2002)
7. Chen, D., Lin, Y., Zhao, G., Ren, X., Li, P., Zhou, J., Sun, X.: Topology-imbalance learning for semi-supervised node classification. *Advances in Neural Information Processing Systems* **34**, 29885–29897 (2021)
8. Chen, J., Xu, Q., Yang, Z., Cao, X., Huang, Q.: A unified framework against topology and class imbalance. In: Proceedings of the 30th ACM International Conference on Multimedia. pp. 180–188 (2022)
9. Chen, M., Wei, Z., Huang, Z., Ding, B., Li, Y.: Simple and deep graph convolutional networks. In: International conference on machine learning. pp. 1725–1735. PMLR (2020)
10. Cui, Y., Jia, M., Lin, T.Y., Song, Y., Belongie, S.: Class-balanced loss based on effective number of samples. In: Proceedings of the IEEE/CVF conference on computer vision and pattern recognition. pp. 9268–9277 (2019)
11. Cui, Y., Jia, M., Lin, T.Y., Song, Y., Belongie, S.: Class-balanced loss based on effective number of samples. In: Proceedings of the IEEE/CVF conference on computer vision and pattern recognition. pp. 9268–9277 (2019)
12. Duan, Y., Liu, X., Jatowt, A., Yu, H.t., Lynden, S., Kim, K.S., Matono, A.: Anonymity can help minority: A novel synthetic data over-sampling strategy on multi-label graphs. In: Machine Learning and Knowledge Discovery in Databases: European Conference, ECML PKDD 2022, Grenoble, France, September 19–23, 2022, Proceedings, Part II. pp. 20–36. Springer (2023)
13. Gao, T., Yao, X., Chen, D.: Simcse: Simple contrastive learning of sentence embeddings. *arXiv preprint arXiv:2104.08821* (2021)
14. Hamilton, W., Ying, Z., Leskovec, J.: Inductive representation learning on large graphs. *Advances in neural information processing systems* **30** (2017)
15. He, K., Chen, X., Xie, S., Li, Y., Dollár, P., Girshick, R.: Masked autoencoders are scalable vision learners. In: Proceedings of the IEEE/CVF conference on computer vision and pattern recognition. pp. 16000–16009 (2022)
16. Hou, Z., Liu, X., Cen, Y., Dong, Y., Yang, H., Wang, C., Tang, J.: Graphmae: Self-supervised masked graph autoencoders. In: Proceedings of the 28th ACM SIGKDD Conference on Knowledge Discovery and Data Mining. pp. 594–604 (2022)
17. Hu, Z., Dong, Y., Wang, K., Chang, K.W., Sun, Y.: Gpt-gnn: Generative pre-training of graph neural networks. In: Proceedings of the 26th ACM SIGKDD International Conference on Knowledge Discovery & Data Mining. pp. 1857–1867 (2020)
18. Huang, C., Li, Y., Loy, C.C., Tang, X.: Learning deep representation for imbalanced classification. In: Proceedings of the IEEE conference on computer vision and pattern recognition. pp. 5375–5384 (2016)
19. Huang, X., Li, J., Hu, X.: Label informed attributed network embedding. In: Proceedings of the tenth ACM international conference on web search and data mining. pp. 731–739 (2017)
20. Jin, S., Zeng, X., Xia, F., Huang, W., Liu, X.: Application of deep learning methods in biological networks. *Briefings in bioinformatics* **22**(2), 1902–1917 (2021)
21. Juan, X., Peng, M., Wang, X.: Exploring self-training for imbalanced node classification. In: Neural Information Processing: 28th International Conference, ICONIP

2021, Sanur, Bali, Indonesia, December 8–12, 2021, Proceedings, Part V 28. pp. 28–36. Springer (2021)

22. Kingma, D.P., Ba, J.: Adam: A method for stochastic optimization. In: Bengio, Y., LeCun, Y. (eds.) 3rd International Conference on Learning Representations, ICLR 2015, San Diego, CA, USA, May 7–9, 2015, Conference Track Proceedings (2015), <http://arxiv.org/abs/1412.6980>
23. Kingma, D.P., Welling, M.: Auto-encoding variational bayes. arXiv preprint arXiv:1312.6114 (2013)
24. Kipf, T.N., Welling, M.: Variational graph auto-encoders. NIPS Workshop on Bayesian Deep Learning (2016)
25. Kipf, T.N., Welling, M.: Semi-supervised classification with graph convolutional networks. In: International Conference on Learning Representations (ICLR) (2017)
26. Li, B., Liu, Y., Wang, X.: Gradient harmonized single-stage detector. In: Proceedings of the AAAI conference on artificial intelligence. vol. 33, pp. 8577–8584 (2019)
27. Li, X., Sun, X., Meng, Y., Liang, J., Wu, F., Li, J.: Dice loss for data-imbalanced nlp tasks. arXiv preprint arXiv:1911.02855 (2019)
28. Lin, T.Y., Goyal, P., Girshick, R., He, K., Dollár, P.: Focal loss for dense object detection. In: Proceedings of the IEEE international conference on computer vision. pp. 2980–2988 (2017)
29. Ma, C., An, J., Bai, X.E., Bao, H.Q.: Attention and cost-sensitive graph neural network for imbalanced node classification. In: 2022 IEEE International Conference on Networking, Sensing and Control (ICNSC). pp. 1–6. IEEE (2022)
30. Ma, Y., Tian, Y., Moniz, N., Chawla, N.V.: Class-imbalanced learning on graphs: A survey. arXiv preprint arXiv:2304.04300 (2023)
31. Ommi, Y., Yousefabadi, M., Faez, F., Sabour, A., Soleymani Baghshah, M., Rabiee, H.R.: Cegg: A deep autoregressive model for class-conditional graph generation. In: Companion Proceedings of the Web Conference 2022. pp. 1092–1098 (2022)
32. Pan, S., Hu, R., Long, G., Jiang, J., Yao, L., Zhang, C.: Adversarially regularized graph autoencoder for graph embedding (2019)
33. Park, J., Lee, M., Chang, H.J., Lee, K., Choi, J.Y.: Symmetric graph convolutional autoencoder for unsupervised graph representation learning. In: Proceedings of the IEEE/CVF International Conference on Computer Vision (ICCV) (October 2019)
34. Park, J., Song, J., Yang, E.: Graphens: Neighbor-aware ego network synthesis for class-imbalanced node classification. In: International Conference on Learning Representations (2021)
35. Qu, L., Zhu, H., Zheng, R., Shi, Y., Yin, H.: Imgagn: Imbalanced network embedding via generative adversarial graph networks. In: Proceedings of the 27th ACM SIGKDD Conference on Knowledge Discovery & Data Mining. pp. 1390–1398 (2021)
36. Radford, A., Kim, J.W., Hallacy, C., Ramesh, A., Goh, G., Agarwal, S., Sastry, G., Askell, A., Mishkin, P., Clark, J., et al.: Learning transferable visual models from natural language supervision. In: International conference on machine learning. pp. 8748–8763. PMLR (2021)
37. Ramesh, A., Dhariwal, P., Nichol, A., Chu, C., Chen, M.: Hierarchical text-conditional image generation with clip latents. arXiv preprint arXiv:2204.06125 (2022)
38. Shchur, O., Mumme, M., Bojchevski, A., Günnemann, S.: Pitfalls of graph neural network evaluation. arXiv preprint arXiv:1811.05868 (2018)
39. Song, J., Park, J., Yang, E.: TAM: Topology-aware margin loss for class-imbalanced node classification. In: Chaudhuri, K., Jegelka, S., Song, L., Szepesvari, C., Niu,

G., Sabato, S. (eds.) Proceedings of the 39th International Conference on Machine Learning. Proceedings of Machine Learning Research, vol. 162, pp. 20369–20383. PMLR (17–23 Jul 2022), <https://proceedings.mlr.press/v162/song22a.html>

40. Tian, Y., Dong, K., Zhang, C., Zhang, C., Chawla, N.V.: Heterogeneous graph masked autoencoders. arXiv preprint arXiv:2208.09957 (2022)
41. Wu, L., Lin, H., Tan, C., Gao, Z., Li, S.Z.: Self-supervised learning on graphs: Contrastive, generative, or predictive. IEEE Transactions on Knowledge and Data Engineering (2021)
42. Wu, L., Xia, J., Gao, Z., Lin, H., Tan, C., Li, S.Z.: Graphmixup: Improving class-imbalanced node classification by reinforcement mixup and self-supervised context prediction. In: Machine Learning and Knowledge Discovery in Databases: European Conference, ECML PKDD 2022, Grenoble, France, September 19–23, 2022, Proceedings, Part IV. pp. 519–535. Springer (2023)
43. You, J., Liu, B., Ying, Z., Pande, V., Leskovec, J.: Graph convolutional policy network for goal-directed molecular graph generation. Advances in neural information processing systems **31** (2018)
44. You, J., Ying, R., Ren, X., Hamilton, W., Leskovec, J.: Graphrnn: Generating realistic graphs with deep auto-regressive models. In: International conference on machine learning. pp. 5708–5717. PMLR (2018)
45. Zeng, L., Li, L., Gao, Z., Zhao, P., Li, J.: Imgcl: Revisiting graph contrastive learning on imbalanced node classification. arXiv preprint arXiv:2205.11332 (2022)
46. Zhang, H., Cisse, M., Dauphin, Y.N., Lopez-Paz, D.: mixup: Beyond empirical risk minimization. arXiv preprint arXiv:1710.09412 (2017)
47. Zhao, T., Zhang, X., Wang, S.: Graphsmote: Imbalanced node classification on graphs with graph neural networks. In: Proceedings of the 14th ACM international conference on web search and data mining. pp. 833–841 (2021)
48. Zhou, D., He, J., Yang, H., Fan, W.: Sparc: Self-paced network representation for few-shot rare category characterization. In: Proceedings of the 24th ACM SIGKDD International Conference on Knowledge Discovery & Data Mining. pp. 2807–2816 (2018)
49. Zhu, Y., Xu, Y., Yu, F., Liu, Q., Wu, S., Wang, L.: Deep graph contrastive representation learning. arXiv preprint arXiv:2006.04131 (2020)